

# CLASP2: The Chromospheric Layer Spectro-Polarimeter

D.E.McKenzie (NASA-MSFC), R.Ishikawa (NAOJ), J.Trujillo Bueno (IAC), F.Auchere (IAS), L.Rachmeler (NASA-MSFC), M.Kubo (NAOJ), K.Kobayashi (NASA-MSFC), A.Winebarger (NASA-MSFC), C.Bethge (USRA), N.Narukage (NAOJ), R.Kano (NAOJ), S.Ishikawa (JAXA), B.dePontieu (LMSL), M.Carlsson (UiO), M.Yoshida (NAOJ), L.Belluzzi (IRSOL), J.Stepan (Ondrejov), T.del Pino Aleman (IAC), E.Alsina Bellester (IAC), A.Asenso Ramos (IAC)

## Scientific Motivation

A major remaining challenge for heliophysics is to decipher the magnetic structure of the chromosphere, due to its “large role in defining how energy is transported into the corona and solar wind” (NASA’s *Heliophysics Roadmap*). Recent observational advances enabled by the Interface Region Imaging Spectrometer (*IRIS*) have revolutionized our view of the critical role this highly dynamic interface between the photosphere and corona plays in energizing and structuring the outer solar atmosphere. Despite these advances, a major impediment to better understanding the solar atmosphere is our lack of empirical knowledge regarding the direction and strength of the magnetic field in the upper chromosphere. Such measurements are crucial to address several major unresolved issues in solar physics: for example, to constrain the energy flux carried by the Alfvén waves propagating through the chromosphere (De Pontieu et al., 2014), and to determine the height at which the plasma  $\beta = 1$  transition occurs, which has important consequences for the braiding of magnetic fields (Cirtain et al., 2013; Guerreiro et al., 2014), for propagation and mode conversion of waves (Tian et al., 2014a; Straus et al., 2008) and for non-linear force-free extrapolation methods that are key to determining what drives instabilities such as flares or coronal mass ejections (e.g., De Rosa et al., 2009).

The most reliable method used to determine the solar magnetic field vector is the observation and interpretation of polarization signals in spectral lines, associated with the Zeeman and Hanle effects. Magnetically sensitive ultraviolet spectral lines formed in the upper chromosphere and transition region provide a powerful tool with which to probe this key boundary region (e.g., Trujillo Bueno, 2014). Probing the magnetic nature of the chromosphere requires measurement of the Stokes  $I$ ,  $Q$ ,  $U$  and  $V$  profiles of the relevant spectral lines (of which  $Q$ ,  $U$  and  $V$  encode the magnetic field information).

## Heritage and New Questions from CLASP1

In September 2015, the CLASP sounding rocket mission successfully made high-sensitivity spectropolarimetric observations of the hydrogen Lyman- $\alpha$  line at 121.6 nm on the solar disk. This spectral line originates in the upper chromosphere and the transition region and its line-center linear polarization signals are sensitive, via the Hanle effect, to magnetic fields with strengths  $10 < B < 100$  G. The data from that first flight (“CLASP1”) showed that the Lyman- $\alpha$  linear polarization produced by scattering processes in the solar atmosphere is of order 1% in the wings and of order 0.1% in the core, and that both have conspicuous spatial variations on scales of  $10'' - 20''$  (Kano et al., in prep.; see more detailed presentations at this Workshop). The scattering polarization signals observed by CLASP1 in the Lyman- $\alpha$  line are consistent with theoretical predictions of line-center  $Q/I$  and  $U/I$  signals of the order of 0.1% (Trujillo Bueno et al., 2011, 2012), of sizable  $Q/I$  wing signals showing a clear center-to-limb variation (CLV; Belluzzi et al., 2012), and of spatial variations caused by the horizontal inhomogeneities of the solar chromospheric plasma (Štěpán et al., 2015).

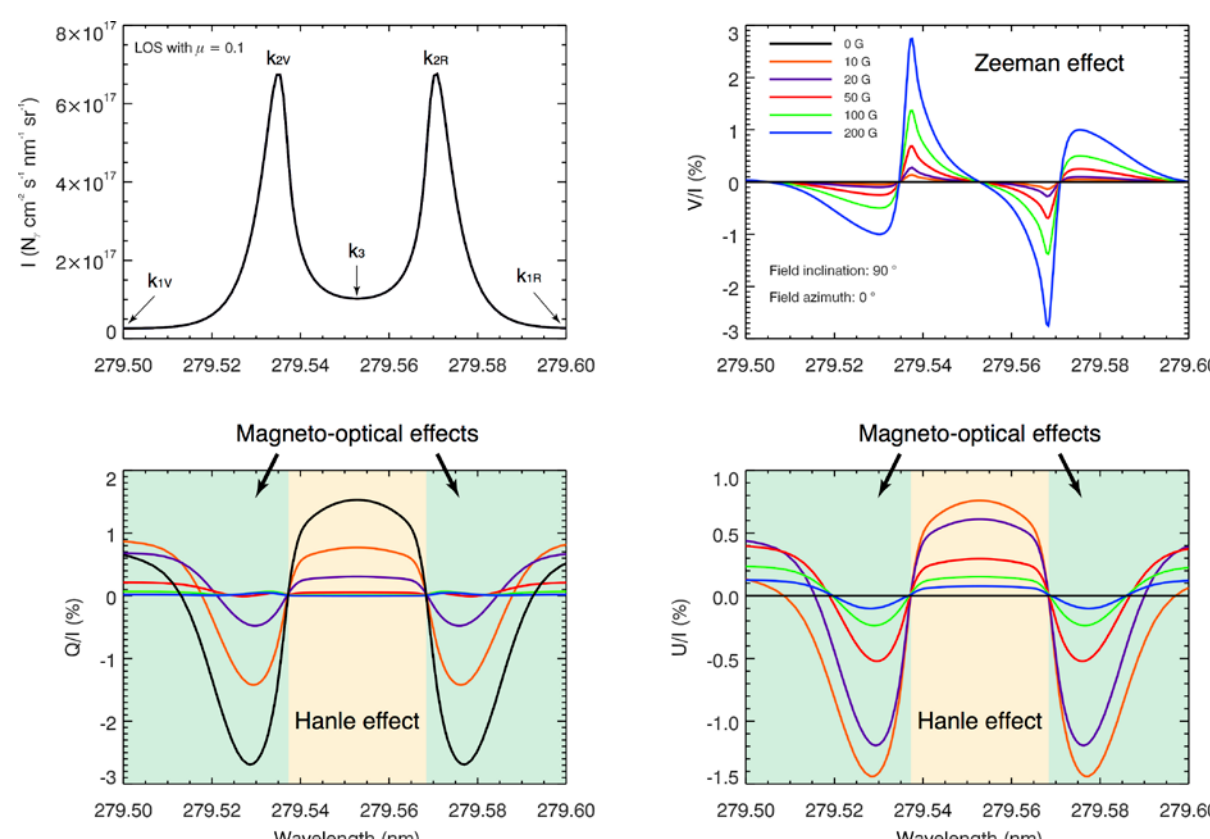
On the other hand, CLASP1 revealed that the observed Lyman- $\alpha$  line-center  $Q/I$  signal does not show any clear CLV, apparently contradicting calculations using available 1D and 3D models of the solar atmosphere. The lack of CLV in the observed line-center  $Q/I$  signal can be explained either by the presence of a significant magnetization in the chromosphere-corona transition region or by the very complex geometry of this boundary region (Trujillo Bueno et al., in prep.; Štěpán et al., in prep.). In addition, CLASP1 revealed that the Si III line at 120.65 nm shows scattering polarization of a few percent (Ishikawa et al., in prep.), and it is notable that this line is sensitive to the Hanle effect for field strengths of  $60 < B < 600$  G. The Si III line and the Lyman- $\alpha$  core and wings have different magnetic sensitivities, and comparison of their scattering polarization signals strongly suggests the operation of the Hanle effect due to the presence of  $\sim 50$  G magnetic fields in network regions (Ishikawa et al., in prep.). These results emphasize the importance of simultaneous spectro-polarimetric observations in UV lines with different magnetic sensitivities.

## Building on CLASP1 heritage

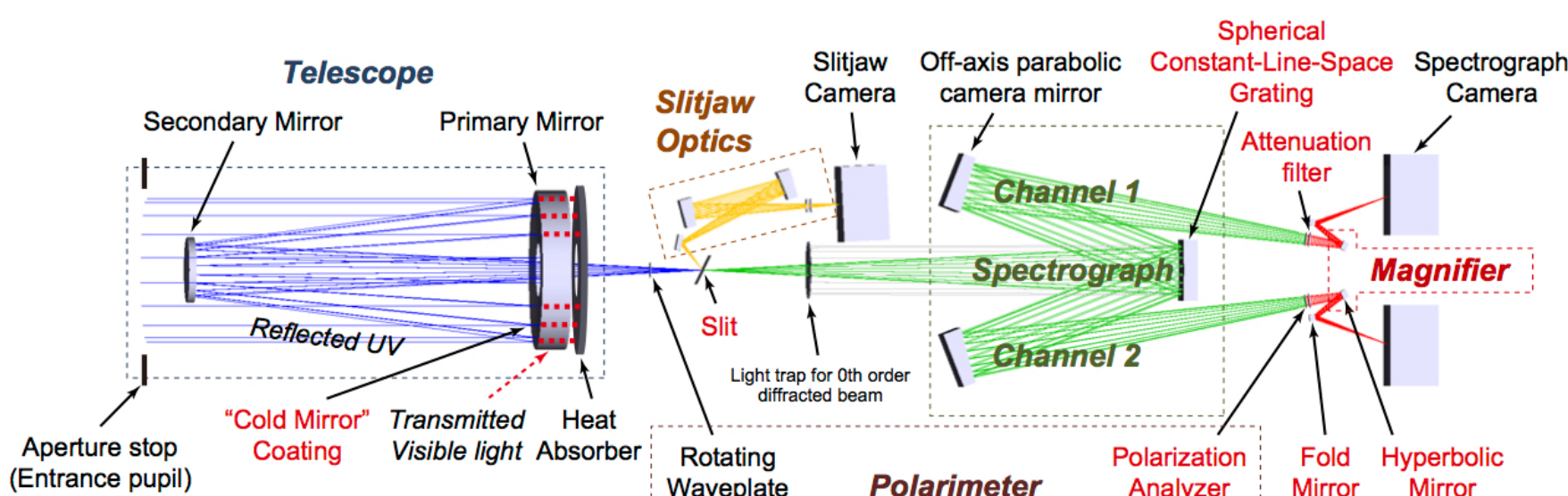
Notwithstanding the achievements of CLASP1, Lyman- $\alpha$  is only one of the magnetically sensitive lines in the UV spectrum; the Mg II  $h$  and  $k$  spectral lines near 280 nm, whose cores form about 100 km below the Lyman- $\alpha$  core, are also a compelling target (Belluzzi & Trujillo Bueno, 2012). This is because they are sensitive to a larger range of field strengths than Lyman- $\alpha$ , through both the Hanle and Zeeman effects. Studying the polarization of the Mg II resonance lines is also particularly timely since their intensity spectrum has been so extensively studied over the past few years with IRIS and via advanced numerical models.

The presence of the magnetic field modifies both the linear and circular polarization signals through the Hanle and Zeeman effects, as illustrated above. The Hanle effect operates at the center of the  $k$  line, around  $k_3$ . Below 50 G, the amplitudes are modified by more than 0.1% when the field strength is increased by 10 G. Differences in field inclination (not shown here) impart modification of the line-center  $Q/I$  and  $U/I$  of order 0.1%. The same panels show also the magnetic sensitivity of the near-wing signals (see the green shaded areas, which include the  $k_{2\theta}$  and  $k_{2\theta}$  peaks) due to magneto-optical effects appearing in the radiative transfer equations for Stokes  $Q$  and  $U$ . The Zeeman-induced circular polarization (Stokes  $V$ ) of the Mg II  $k$  line is illustrated in the upper right-hand panel of the figure; similar  $V/I$  profiles are obtained for the  $h$  line. For a longitudinal field of 50 G the Zeeman effect produces  $V/I$  signals of about 0.5% in the Mg II  $k$  line. It is also notable that the circular polarization in the (blended) subordinate line of Mg II at 279.8 nm (not shown), is also significant. This subordinate line is sensitive to heating in the low chromosphere (Pereira et al., 2015), and provides an additional probe of the thermal and magnetic conditions in the atmosphere (Belluzzi & Trujillo Bueno, 2012).

Therefore, to make progress towards a better understanding of the solar chromosphere, CLASP2 will measure the wavelength variation of all four Stokes parameters in the spectral region between 279.45 nm and 280.35 nm, specifically in Mg II lines sensitive to the physical conditions of the solar atmosphere throughout a diagnostically important range of heights.



The Stokes profiles of the Mg II  $k$  line calculated for a position close to the limb ( $\mu = 0.1$ ) in a semi-empirical model of the solar atmosphere, in the absence and in the presence of a horizontal magnetic field with azimuth  $\chi_B = 0^\circ$  (i.e., on the plane defined by the local vertical and the line of sight).

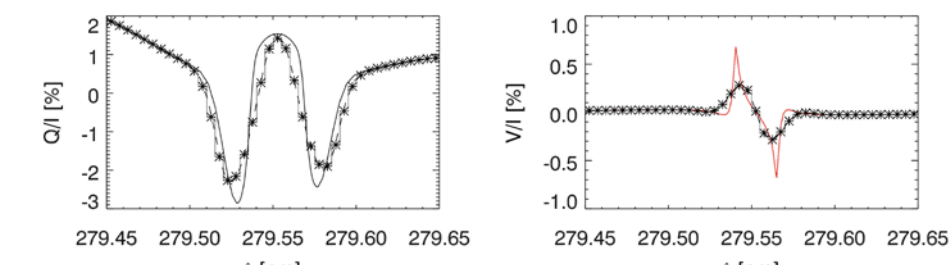


## The CLASP Telescope, Modified for Mg II

The CLASP instrument was originally designed for studying H Lyman- $\alpha$  (Narukage et al., 2015). For CLASP2, we will reuse it with minor modifications to observe the Mg II lines near 280 nm. The instrument consists of a Cassegrain telescope, a dual-beam spectrograph assembly with a grating serving as a beam splitter, a polarimeter including a rotating waveplate and an identical pair of transmissive polarization analyzers, and a slitjaw imaging system. The overall layout and baseline design parameters are shown in the figure above. The optical elements that will be updated for CLASP2 are indicated by the red text in the figure.

The polarimeter system consists of a rotating waveplate and two transmissive polarization analyzers. The rotating waveplate allows measurement of Stokes  $Q$ ,  $U$ , and  $V$  with fixed polarization analyzers. The optical components between the waveplate and the polarization analyzers are oriented to minimize polarization errors and crosstalk: the ruling of the diffraction grating is parallel or perpendicular to the polarization axis of the polarizers, and the mirrors downstream of the grating are tilted around the same axis. These configurations were adopted for CLASP1; an end-to-end polarization calibration of the spectropolarimeter system verified that the residual  $Q \leftrightarrow U$  crosstalk corresponded to an azimuth error of  $< 0.5^\circ$  (Ishikawa et al., 2014; Giono et al., 2016b).

We have considered the impact of the spectral resolution on the polarization signatures by convolving the calculated Stokes profiles with Gaussian functions of different widths. A spectral resolution of at least 0.01 nm is sufficient to recover the line-core  $Q/I$  and  $U/I$  signals without significant deterioration, and to detect the antisymmetric  $V/I$  signals for longitudinal fields as low as 50 G (see figure below).



Left: Theoretical estimate of the  $Q/I$  signals in Mg II  $k$  [nm] produced by scattering processes in the upper solar chromosphere. Right: The Zeeman-induced wavelength variation of  $V/I$  around the Mg II  $k$  line, taking into account the Zeeman effect of a longitudinal magnetic field of 50 G. The solid lines correspond to the pure theoretical solutions. Dashed curves include the effect of spectral smearing by convolving with a Gaussian with  $2\sigma = 0.01$  nm. The asterisks consider a spectral sampling of 0.005 nm/pix, resulting in an effective wavelength resolution of 0.01 nm (Nyquist limited).

## Acquisition and Demodulation

**CLASP2 is proposed for a sounding rocket flight in the spring of 2019.** During flight we will observe three targets. The first is at disk center for polarization calibration. Second, we will target a strong-field ( $> 50$  G) region, such as plage, to constrain the three components of the magnetic field by measuring the full Stokes vector. Finally we will position the slit perpendicular to the limb, sampling a quiet region, and with the slit extending  $20''$  above the limb. This last target enables investigation of the CLV in linear polarization in the center of the Mg II  $k$  line (sensitive to the Hanle effect) and in the wings of the Mg II  $h$  &  $k$  lines (sensitive to the magneto-optical effects). Ideally, if solar conditions allow, the heliocentric angles of the plage and quiet region will be similar to facilitate comparison of their measurements. A slit length of  $200''$  is adequate to quantify the CLV across the quiet Sun target, and also provides sufficient sampling of a plage region.

All the raw data are returned without onboard processing; demodulation will be done on the ground using all of the flight data. First, we derive fractional polarizations ( $Q/I$ ,  $U/I$  and  $V/I$ ) using only the data from a single channel. Every successive set of 16 images of the data, corresponding to one rotation of the waveplate, will cancel out non-uniformities in the waveplate and fringe patterns caused by the waveplate. The Stokes signals from one channel will be verified by comparing to those from the other channel, and both signals will be summed to obtain the final Stokes profiles after calibration and alignment of the two channels. This procedure cancels possible polarization errors in the single-channel demodulation caused by time variation of source intensity and time variation of instrument pointing since the two channels take orthogonal pairs of polarization simultaneously.

The table below demonstrates the flowdown of requirements from the science objectives to the CLASP2 instrument capabilities.

Science Objective Question: What is the magnitude of the magnetization and geometrical complexity of the upper chromosphere in quiet and plage regions?		
Scientific Measurements	Scientific Requirements	Instrument requirements
M1: In center of an upper chromospheric line that is sensitive to the Hanle effect, measure variations in the linear polarization due to scattering and the Hanle effect.	R1: Spectrally resolve the linear polarization (Stokes $Q/I$ and $U/I$ ) in the center of Mg II $k$ .	Observational Targets, from R1, R3, R5,
	R2: Perform measurements along a spectrograph slit with adequate spatial resolution to resolve solar features.	Slit length 200 arcsec, from R2, R5
	R3: Sample the Sun in strong-field regions and from the center to the limb in quiet regions.	Polarization sensitivity 0.1% for $Q/I$ & $U/I$ in core, from R1 0.3% for $Q/I$ & $U/I$ in wings, from R6 0.1% for $V/I$ in core, from R4 (core = between $k_2/k_2$ peaks)
M2: Measure the circular polarization in an upper chromospheric line that is sensitive to the Zeeman effect.	R4: Spectrally resolve circular polarization (Stokes $V/I$ ) in Mg II $h$ & $k$ .	Spectral resolution 0.01 nm, from R1, R4
	R5: Sample strong-field solar structures (such as plage) with adequate spatial resolution.	Wavelength range 279.45 to 280.35 nm, from R1, R4, R6
M3: In the wings of an upper chromospheric line, measure linear polarization due to scattering and (Zeeman) magneto-optical effects.	R6: Observe a spectral window large enough to include the Stokes $Q$ and $U$ wings of Mg II $h$ & $k$ .	Spatial resolution Strong Field region: 2 arcsec, from R5 Quiet Sun region: 10 arcsec, from R2
		Temporal resolution A single measurement is needed at each pointing satisfying the requirements above; from R2, R5

## References

- Belluzzi, L., & Trujillo Bueno, J., 2012. The Polarization of the Solar Mg II  $h$  and  $k$  Lines. *ApJ*, 750:L11.
- Belluzzi, L., Trujillo Bueno, J., & Štěpánek, J., 2012. The Scattering Polarization of the Ly $\alpha$  Lines of H I and He II Taking into Account Partial Frequency Redistribution and J-state Interference Effects. *ApJ*, 755:L2.
- Cirtain, J. W., Golub, L., Winebarger, A. R., de Pontieu, B., et al., 2013. Energy release in the solar corona from spatially resolved magnetic braids. *Nature*, 493:501.
- de Pontieu, B., Rouppe van der Voort, L., McIntosh, S. W., Pereira, T. M. D., et al., 2014. On the prevalence of small-scale twist in the solar chromosphere and transition region. *Science*, 346:1255732.
- De Rosa, M. L., Schrijver, C. J., Barnes, G., Leka, K. D., et al., 2009. A Critical Assessment of Nonlinear Force-Free Field Modeling of the Solar Corona for Active Region 10953. *ApJ*, 696:1780.
- Giono, G., Ishikawa, R., Narukage, N., Kano, R., et al., 2016b. Polarization calibration of the Chromospheric Lyman-Alpha SpectroPolarimeter for a 0.1% polarization sensitivity in the VUV range. Part I: Pre-flight calibration. *Sol. Phys.*, in press.
- Guerreiro, N., Haberreiter, M., Schmutz, W., & Hansteen, V., 2014. Identification and characterization of small-scale heating events in the solar atmosphere from 3D MHD simulations. In 40th COSPAR Scientific Assembly, COSPAR Meeting, volume 40, page 1095.
- Ishikawa, R., Narukage, N., Kubo, M., Ishikawa, S., Kano, R., & Tsuneta, S., 2014. Strategy for Realizing High-Precision VUV Spectro-Polarimeter. *Solar Physics*, 289(1):4727.
- Narukage, N., Auchére, F., Ishikawa, R., Kano, R., et al., 2015. Vacuum ultraviolet spectropolarimeter design for precise polarization measurements. *Appl. Opt.*, 54:2080.
- Straus, T., Fleck, B., Jefferies, S. M., Cauzza, G., et al., 2008. The Energy Flux of Internal Gravity Waves in the Lower Solar Atmosphere. *ApJ*, 681:L125.
- Tian, H., DeLuca, E., Reeves, K. K., McKillop, S., et al., 2014a. High-resolution Observations of the Shock Wave Behavior for Sunspot Oscillations with the Interface Region Imaging Spectrograph. *ApJ*, 786:137.
- Trujillo Bueno, J., Štěpánek, J., & Belluzzi, L., 2012. The Ly $\alpha$  Lines of H I and He II: A Differential Hanle Effect for Exploring the Magnetism of the Solar Transition Region. *ApJ*, 746:L9.
- Trujillo Bueno, J., Štěpánek, J., & Casini, R., 2011. The Hanle Effect of the Hydrogen Ly $\alpha$  Line for Probing the Magnetism of the Solar Transition Region. *ApJ*, 738:L11.